Anal. Chem. **2001,** *73,* 3662−3668

Chemical Plume Tracking. 1. Chemical Information Encoding

Timo Kikas, Hiroshi Ishida,† Donald R. Webster,‡ and Jiří Janata*

School of Chemistry and Biochemistry, Georgia Institute of Technology, Atlanta, Georgia 30332-0400

It is shown experimentally that chemical information can be encoded and preserved in flowing liquid streams. It can be retrieved by chemical sensing arrays using correlation analysis. This finding is important for understanding of the mechanism of chemotaxis as practiced by some aquatic animals and also is a necessary prerequisite for construction of chemical plume tracking robots.

In the search for food or mates, or to elude predators, aquatic animals have developed successful navigational strategies that depend on tracking chemical signals.[1,2] Understanding these strategies is a desirable goal that would have impact on the construction of engineered searchers and their use in pollution control, in natural resource exploration, or even in the area of military defense.

Some marine animals have their olfactory sensors distributed along their appendages.[3] They can be viewed as "model" searchers for tracking chemical signals in an aqueous environment. Conversely, an array of eight microelectrodes can be viewed as a corresponding "engineered" searcher. Amperometric microelectrodes transduce rapidly and linearly the local instantaneous concentration of the electroactive marker into an electrical signal. Therefore, an assembly of eight microelectrodes (Figure 1) can be accepted as the geometrically reasonable sensor array model of the olfactory system of some marine animals.

The turbulent chemical plumes are complex, dynamic fields of chemical concentrations.[4,5] Their structure is commonly studied by laser-induced fluorescence (LIF). In this technique, the sheet of laser radiation excites the fluorescent marker injected from a nozzle and a CCD camera perpendicular to the laser sheet registers the fluorescent intensity.[6] Any point selected in such record can be viewed as a "virtual optical sensor" located at that point.

The ultimate goal of this study is to characterize a form of the animal search algorithm and to adopt it for the "engineered" searcher. There are two immediate questions that need to be addressed in order to achieve this goal. The first is, "how is the chemical information encoded and maintained in the turbulent flow"? The second question is, "how is this information interpreted by the animal?" A successful search strategy means that the location of the odor source is done with the minimum expenditure of energy.[7] Answers to both questions are quite complex. This study attempts to address only the first question: the nature of encoding/readout of the chemical information in turbulent plumes. To further simplify the task, the information encoding has been studied first with only one pair of sensors and in a constrained laminar flow (part 1). In the second part, the study has been extended to include controlled turbulence. It has been suggested[8,9] that temporal analysis of chemical signals may be the key to designing search strategies for engineered robots. With the aid of a benchtop fluidic system, we try to extend this notion by examining the most elementary aspects of chemical sensing. We also want to show that the chemical sensing arrays open a new dimension in chemical sensing of these complex concentration fields.

THEORY

The Signal. In a steady-state turbulent plume, at any point located at distance L from the source, the instantaneous concentration $C(t)$ of the marker can be expressed as the sum of the mean value $\langle C \rangle$ and of the fluctuating concentration $c(t)$

$$C(t) = \langle C \rangle + c(t) \tag{1}$$

The sensing signal $x(t)$ is directly proportional to the product of concentration of the odorant $C(t)$ and of the mass transport coefficient m

$$x(t) = km\{\langle C \rangle + C(t)\} \tag{2}$$

The proportionality constant, k, depends on the sensing principle used. For amperometric sensors, k contains the usual constants: the area of the electrode, the number of electrons exchanged, and the Faraday charge. On the other hand, the mass transport coefficient, m, depends on the size and shape of the electrode, which determine the mode of mass transport, and on the orientation of the electrode with respect to the mean flow vector.

* Corresponding author: (phone) (404) 894 4828; (fax) (404) 894 8146; (e-mail) jiri.janata@chemistry.gatech.edu.

† Present address: Department of Physical Electronics, Tokyo Institute of Technology, 2-12-1 Ookayama, Meguro-ku, Tokyo 152-8552, Japan.

‡ School of Civil and Environmental Engineering, Georgia Insitute of Technology.

(1) Weissburg, M. J.; Zimmer-Faust, R. K. *Ecology* **1993**, *74*, 1428−1443.
(2) Basil, J.; Atema, J. *Biol. Bull.* **1994**, *187*, 272−273.
(3) Derby, C. D.; Atema, J. () *J. Exp. Biol.* **1982**, *98*, 303−315.
(4) Fackrell, J. E.; Robbins, A. G. *J. Fluid Mech.* **1982**, *117*, 1−26.
(5) Shraiman, B. I.; Siggia, E. D. *Nature* **2000**, *405*, 639−646.
(6) Webster, D. R.; Weissburg, M. *J. Limnol. Oceanog.* In press.
(7) Dusenbery, D. B. *J. Chem. Ecol.* **1989**, *15*, 2511−2519.
(8) Atema, J. *Proc. Natl. Acad. Sci. U.S.A.* **1995**, *92*, 62−66,
(9) Ishida, H.; Nakamoto T.; Moriizumi, T.; Kikas, T.; Janata, J. *Biol. Bull.* **2000**, *200*, 222−226.

10.1021/ac0101813 CCC: $20.00
Published on Web 07/06/2001

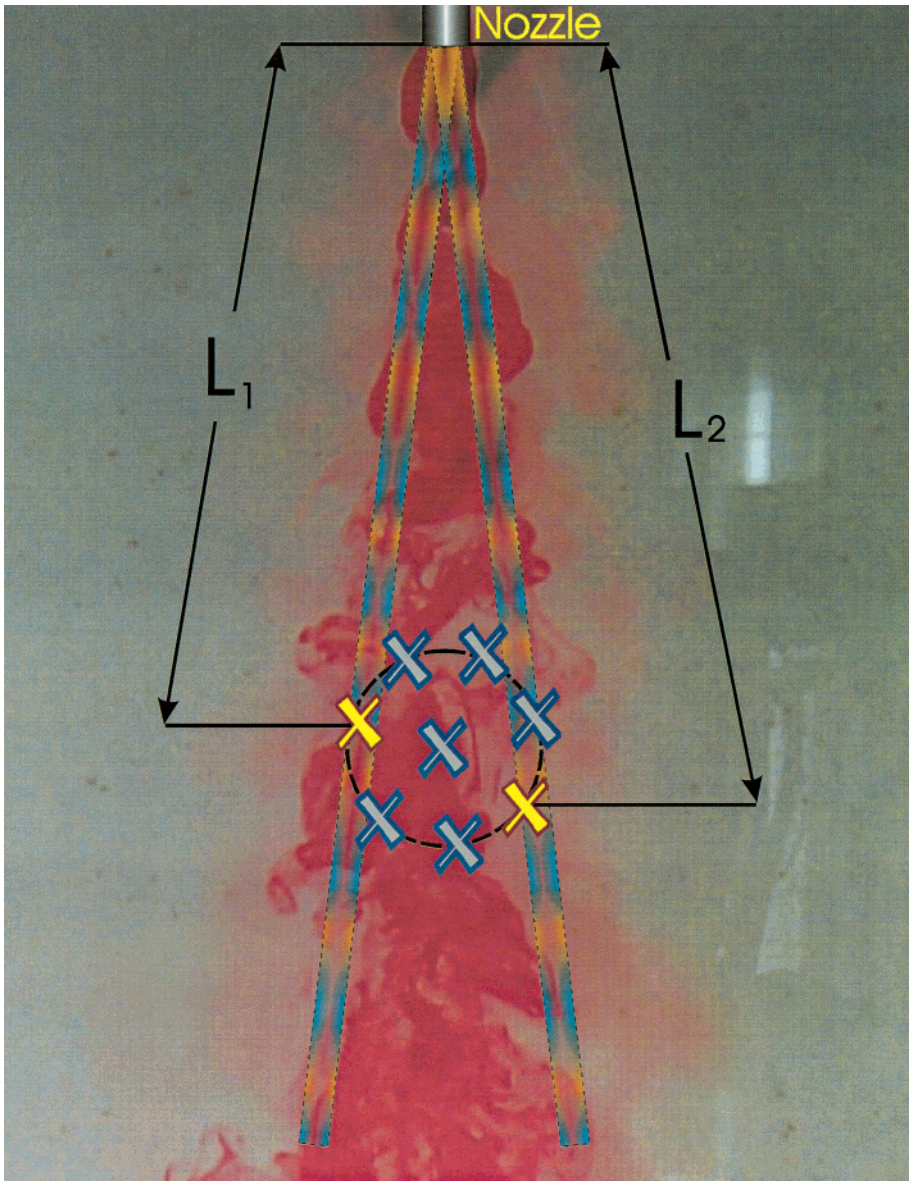

Figure 1. Visualization of the chemical plume. Photograph of red dye isokinetically injected into a fully developed turbulent boundary layer with average flow velocity of 5 cm/s. The position of the hypothetical eight-sensor array in the chemical plume is shown by X-marks. The pair of sensors used in the correlation analysis is highlighted. They are L_1 and L_2 cm away from the source. The overlaid stripes represent two channels realized in the benchtop virtual plume.

Most importantly, it depends on the instantaneous value of the flow rate. Thus, the magnitude of the overall amperometric signal fluctuates both with concentration and with flow. The signal from sensors that do not depend on mass transport, such as equilibrium potentiometric or optical sensors, are flow-independent. For example, the information obtained from the "virtual optical sensor" by the LIF approach does not depend on m and can be used to obtain the instantaneous local concentration values. While optical sensing is not an obvious option for most marine animals that rely on *contact* olfactory sensors, it may be a viable option for engineered robotic sensors. Therefore, the biological plume tracking models, as useful and instructional as they are, should not become the constraining factor on the overall plume-tracking project.

The examination of the snapshot of the chemical plume (Figure 1) suggests a complex pattern of fluctuating concentration at the eight points that have been selected to model a sensing array arbitrarily placed in the plume concentration field. Here we present a hypothesis that the navigational information provided by such array (or perhaps also by the marine animals) is contained in the *fluctuating part x(t)* of the signal (eq 2). From a chemical sensing point of view, this paradigm explores a new dimension in sensing—correlation analysis of the temporal fluctuations in concentration across spatially separated elements of chemical sensing arrays. The outline of such analysis is presented in the following section. A more detailed treatment of this approach will be published separately in the paper describing the analysis of the LIF plume data.[10]

Correlation Analysis of Sensor Array Response. First we assume that the source of the chemical signal imposes some periodic fluctuation of concentration of the marker. This is a realistic assumption since a physical object (i.e., a cylinder) placed

(10) Ishida, H.; Webster, D. R.; Kikas, T.; Janata J. Manuscript in preparation.

in the flowing stream generates eddies whose frequency, f_s, is related to the flow velocity V, diameter D, and its shape. A simple empirical formula for f_s is then

$$f_s = S_t(V/D) \tag{3}$$

The Strouhal constant S_t has the value of 0.21 for Reynolds numbers in the range 100−100 000.[11] The eddies frequency modulate the steady release of marker at the source (Figure 1). Therefore, the fluctuating concentration of the marker has a causal relationship with the chemical emission at the source at the specific modulation frequency. Turbulent eddies in the flow dilute the marker *randomly* and appear at the sensors 1 and 2 as *uncorrelated* fluctuations. Thus, the objective of the search exercise based on correlation analysis of this fluctuating field is to locate the source encoded at the *correlated* source frequency f_s. The problem can be rephrased in terms of identifying and locating the correlated signal at a specific frequency in an inherently uncorrelated (i.e., "noisy") fluctuating field. Such problems are common in noise reduction (signal detection) in audio or visual applications. They are often solved with the aid of correlation analysis.[12] As far as we know, this approach has not yet been applied to olfactory analysis and specifically to chemical sensing with arrays of sensors. The necessary condition for performing correlation analysis is the availability of the array of rapidly responding chemical sensors. This is the main reason for selecting fast amperometric microelectrodes and also for using the LIF data as the "virtual optical sensors".

Signal $x(t)$ from each individual sensor in the array has the average power P that is expressed as

$$\langle P \rangle = \frac{1}{ZT_D}\int_0^{T_D} \mathrm{d}t\cdot x^2\,(t) \tag{4}$$

where T_D is the duration of the observation period and Z is the impedance of the system. In a well-behaved amperometric mode of detection, it is implicitly assumed that the current is proportional to the concentration and that this proportionality holds over the experimental bandwith. It should be noted that power is the rate of use (or generation) of energy. Conversely, the energy is the time integral of the power in a given observation period. According to the Parseval theorem,[12] the correlation analysis can be performed either in the time domain or in the frequency domain. In the latter, it allows us to compare and correlate the power in individual sensing frequencies.

The fluctuating electrical signal $x(t)$ resulting from the injection of the marker is a periodic function superimposed on a stationary random noise component induced by turbulence. The dilution of the average marker concentration downstream from the source represents a superimposed function $y(t)$ which can be seen as the power law decay of the energy of the signal $x(t)$. The autocorrelation function $a_f(\tau)$ tells us how much energy of the original signal $x(t)$ remains after the delay time τ

$$a_f(\tau) = \frac{1}{Z2T_D}\int_{-T_D}^{T_D} \mathrm{d}t\cdot x(t)\cdot x(t+\tau) \tag{5}$$

At zero delay time, the average power $\langle P \rangle$ equals the autocorrelation function $a_f(0)$, evaluated at $\tau = 0$. The autocorrelation function is a "double-sided" function and hence the factor 2 in the denominator.

According to the Wiener-Khintchine theorem,[12] the Fourier transform of the autocorrelation function is the *energy spectral density*

$$A_f(\omega) = \frac{1}{Z2T_D}\int_{-T_D}^{T_D} \mathrm{d}t\cdot \mathrm{e}^{-i\omega\tau}\, a_f(\tau) = |X(\omega)|^2 \tag{6}$$

where $X(\omega)$ is the Fourier transform of signal $x(t)$.[13] It measures the amount of energy that is contained in the signal in the frequency range ω and $(\omega + \mathrm{d}\omega)$. Therefore, it is an energy per unit frequency per unit impedance and for electrical signal has the units $(\text{volts})^2\ (\text{ohm})^{-1}\ (\text{hertz})^{-1}$. The Wiener−Khintchine theorem is the statement of equivalency of information in the frequency and in the time domain. The autocorrelation spectral density can be computed for each sensor in the array, yielding $|X_{jj}(\omega)|^2$, $|X_{kk}(\omega)|^2$, etc., where j·k... represent the sensor number.

The cross-correlation function $\gamma_f(\tau)$ defines the relationship between two temporal functions $x(t)$ and $y(t)$

$$\gamma_f(\tau) = \frac{1}{Z2T_D}\int_{-T_D}^{T_D} \mathrm{d}t\cdot x(t)y(t+\tau) \tag{7}$$

and, according to the Wiener−Khintchine theorem, also defines the *cross-power spectral density* $\Gamma_f(\omega)$

$$\Gamma_f(\omega) = X(\omega)\cdot Y(\omega) \tag{8}$$

in terms of the Fourier transform $X(\omega)$ and the complex conjugate $Y(\omega)$ of the functions $x(t)$ and $y(t)$, respectively.[12] In the sensor analysis context, we will be performing cross-correlation between a pair of selected sensors in the array, yielding the cross-power spectral density $|X_{jk}(\omega)|^2$.

Finally, we need to describe another function called *coherence* $\alpha^2(\omega)$. Our study has shown that this function has the highest diagnostic value for chemical plume tracking. It can be used to extract the energy in the common signal between two sensors at any given frequency. It is the square of cross-power spectral density $X_{1,2}(\omega)$ of sensors 1 and 2 divided by the product of the autopower spectral densities from the same sensors

$$\alpha^2(\omega) = \frac{|X_{j,k}(\omega)|^2}{|X_{j,j}(\omega)|\cdot|X_{k,k}(\omega)|} \tag{9}$$

For completely correlated signals, $\alpha^2(\omega) = 1.0$ while for completely uncorrelated signals $\alpha^2(\omega) = 0$. The coherence is defined for the entire range of frequencies. Therefore, it can be interpreted as a *frequency-dependent correlation coefficient.* Unlike auto- and cross-power spectral densities, it is a dimensionless parameter. That is the reason for its remarkable robustness, as has been demon-

(11) White, F. M. *Viscous Fluid Flow*, 2nd ed.; McGraw-Hill: New York, 1991.
(12) Hartmann, W. M. *Signals Sound, and Sensation*; Springer-Verlag: New York, 1998.
(13) The Fourier transform of $x(t)$ is complex number containing both the *real*, $X(\omega)$, and its *imaginary* complex conjugate $X(-\omega) = X(\omega)$.

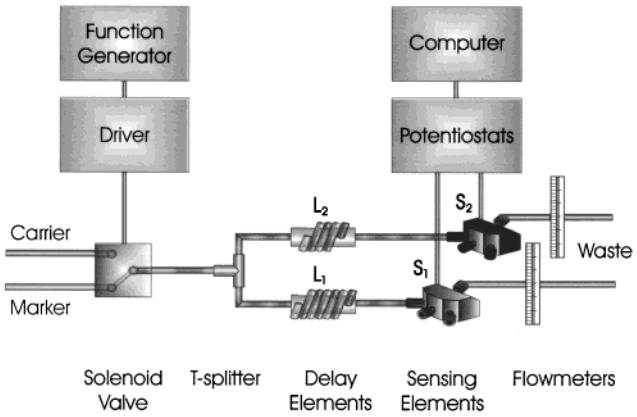

Figure 2. Block schematic of the virtual plume used to study frequency modulation. Lines L_1 and L_2 represent lengths of the delay elements, and S_1 and S_2 represent flow-through chambers housing the amperometric sensors.

strated in this study. In the ideal case, the fully correlated signal modulated at pure sinusoidal frequency f_s is expected to have a coherence value equal to unity at that frequency and zero at all other frequencies. In a nonideal case, the residual between the coherence value and 1.0 is due to the uncorrelated noise in the system and to the uncorrelated distortions introduced by the transducers. In our benchtop experiment, the modulation is achieved by creating series of regular concentration pulses. Since concentration cannot reach a negative value and since the response to the pulse shape is significantly different from the pure sine wave, the system is nonideal by definition. Consequently, a nonzero energy is present also in higher harmonics of the fundamental frequency. The energy at those higher harmonics is clearly discernible in the coherence spectrum while it is less visible in both the auto- and cross-power spectra. The higher harmonics are real physical signals containing some signal energy. Therefore, in the correlation analysis of nonsinusoidal systems, they may also carry some useful information. The detailed analysis of the nonsinusoidal signals and the experimental verification of the information value of higher harmonics will be discussed in part 2 of this series.

EXPERIMENTAL SECTION

To test the viability of the coherence function from a multisensor array, experiments were performed in a controlled benchtop apparatus called the "virtual plume" (VP).[14] The block diagram of the frequency-modulated virtual plume (MVP) is shown in Figure 2. With this system, we examined the effects of flow velocity, spacing, distance, and orientation of the individual sensors. We have also determined the frequency bandwidth of the flowing stream with respect to concentration modulation. It is important to acknowledge that the flow in the virtual plume channels is *constrained laminar*, while *unconstrained turbulence exists* in the real plume. Therefore, any extrapolation of the results obtained from the virtual plume conditions must take this limitation into consideration.

Carrier and sample solutions were delivered at a constant rate with minimum fluctuations in a gravity-driven system. A solenoid three-way isolation valve (Biochem-Valve 075T3) was used to inject the sample plugs with specific frequency that will be referred to as the modulation frequency, f_s. The solenoid valve was controlled by a custom-designed driver circuit. A square waveform was delivered from the waveform generator (Hewlett-Packard 33120A) to activate the solenoid driver circuit. Data were collected for 1000 s with an acquisition frequency of 20 Hz, to avoid aliasing. Data were analyzed using the Matlab software package (Matlab 5.3 for Windows).

The delay elements were designed to provide different retention times for marker plugs while minimizing additional dispersion. Coils of Teflon tubing with inner diameter of 0.5 mm and lengths from 10 to 200 cm were used for this purpose.

The sensing elements consist of platinum microelectrodes housed in the flow-through cells.[14] A three-electrode electrochemical configuration was used in order to prevent polarization of the silver wire reference electrode. A stainless steel outlet tube served as an auxiliary electrode. Electrodes were connected to potentiostats (OMNI 90, Cypress Systems, Inc.), and the signals were interfaced to a PC via a DAC interface card (AT-MIO-16XE-10, National Instruments).

Commercial flow meters/controllers (Accucal flow meter, Gilmont Instruments) with precision flow control valves (14 turns) were used to control the flow rate of different channels. The operating range of the flow meters is 0.0112−4.92 mL/min.

Solutions and Reagents. All solutions were made in 0.482 M NaCl solution in order to mimic the salt concentration in the marine environment and at the same time provide a supporting electrolyte. A 2.5 mM solution of hexaammineruthenium trichloride ($(NH_3)_6RuCl_3$) was used as the electrochemical marker because of its ideal electrochemical behavior.

RESULTS

Experimental Realization of the Fluctuating Concentration Field. The electroactive odorant marker is delivered to the carrier stream as a series of concentration pulses at the modulation frequency, f_s, using the solenoid valve. The stream is divided into two channels of length, L_1 and L_2, containing amperometric sensors 1 and 2. The time sequence of the modulated amperometric current is recorded (Figure 3A). The instability of the "envelope" of the amperometric current evident in Figure 3A shows the undesirable combined effect of concentration *and* flow velocity on the signal. The inset in Figure 3A shows an expanded 1-s segment of the time record. It is evident that in order to perform correlation analysis it is not necessary for the current to reach a "zero" value between the injected concentration pulses. The time sequence is converted to the frequency domain using a standard fast Fourier transformation integral algorithm to yield autopower spectral density for each channel (Figure 3B), $A_{1,1}(\omega)$ and $A_{2,2}(\omega)$, according to eq 6. The cross-power spectral density $\Gamma_{1,2}(\omega)$ (not shown) and coherence $\alpha^2(\omega)$ (Figure 3C) are computed according to the eqs 8 and 9, respectively. This approach has been used to examine the effect of various experimental parameters as discussed below.

Effect of Distance on Frequency Encoding. The most important question is, "if and how far is the frequency-encoded information preserved in the flow?" To answer that question, two-channel signal modulation experiments were conducted using the basic setup described in Figure 2. In these experiments, the length

(14) Kikas, T.; Ishida, H.; Roberts, P. J. W.; Webster, D. R.; Janata, J. *Electroanalysis* **2000**, *12*, 974−979.

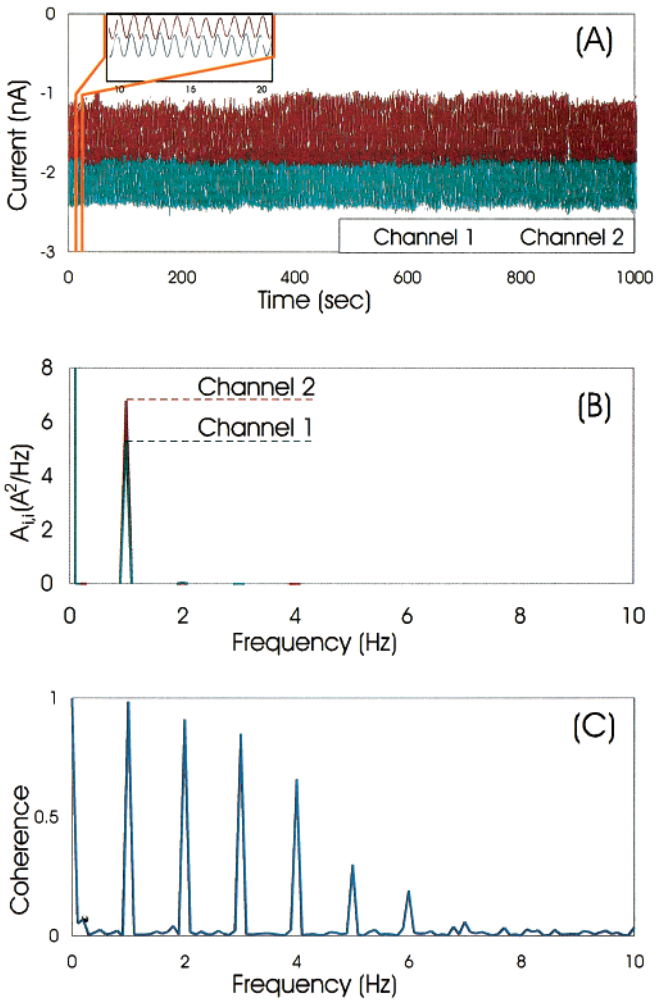

Figure 3. Information in the modulated signal of the virtual plume. (A) The time series for the two-channel flow modulation experiment in the virtual plume. Modulation frequency was 1 Hz, and flow rate was 0.6 mL/min; (B) autopower spectrum densities for both channels calculated from the time series given in (A); (C) coherence between the two channels in the frequency domain for the given time series.

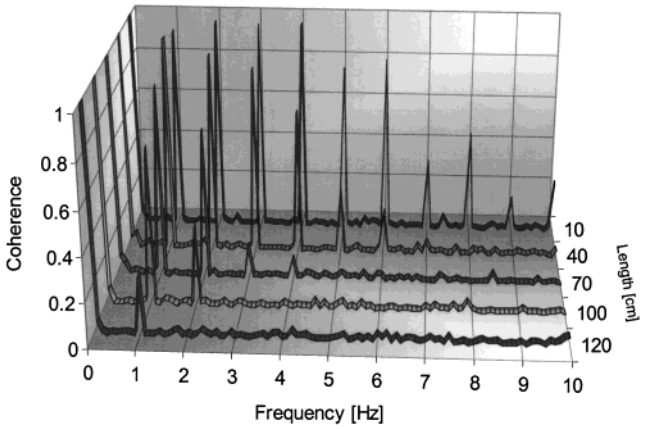

Figure 4. Dependence of the *observed frequency* on the length of the delay element (DeE). Coherence spectra for the different L_1/L_2 pairs are plotted against the L_1 ($L_2 = L_1 + 10$ cm). Modulation frequency was 1 Hz, and flow rate was 0.6 mL/min.

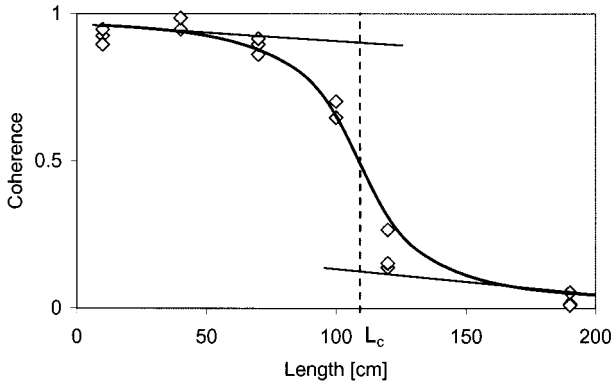

Figure 5. Dependence of the *coherence value* at the fundamental frequency on distance from the source (L_1 was used as the distance of the array from the source). Flow rate in the channels was 0.6 mL/min, and modulation frequency was 1 Hz.

of the delay elements (L_1, L_2) was varied so that the delay element of one channel was always 10 cm longer than the other. The reason for the 10-cm additional delay was to mimic the size of the array (as illustrated in Figure 1). Thus, if the signal in the first channel was what the front sensor of the array would detect, then the signal in the second channel was what the rear sensor of the array would detect. The delay lines were varied from 10 (shorter in this pair) to 200 cm (longer in this pair). The volume flow in both channels was kept constant at ~0.6 mL/min, which corresponds to a linear flow velocity of 5.0 cm/s. The source modulation frequency was 1.0 Hz. Figure 4 shows that the *coherence value* at the fundamental frequency decreases with the increasing length but the *frequency* does not change. That proves that the information encoded by external perturbation into the plume structure (eq 3) should remain encoded for some distance from the source and can be observed at the modulation frequency.

Another important observation can be made about the presence of higher harmonics. They result from nonidealities of the concentration variations, namely, the departure of the concentration variations from pure sinusoidal. The value of coherence at the fundamental and all harmonic frequencies decreases with increasing distance from the source. The coherence values at the modulation frequency were plotted against the length of the shorter delay element in the pair. Figure 5 shows that coherence at the modulation frequency initially stays constant and then starts decreasing with the increasing length of the delay element. The inflex point of this dependence defines a critical length of the delay element (L_c).

Dependence of Frequency and Coherence on Flow. The chemical plume is complex not only structurally but also dynamically. Therefore, the flow velocity in the plume field is not constant. It is essential to ascertain whether the frequency encoded into the plume structure changes with the flow rate. An analogy with the Doppler effect may suggest that higher flow rate would bring the periodically fluctuating concentration in contact with the sensor surface at a *higher rate*, resulting in a higher *perceived* frequency of modulation. On the other hand, chemical marker injected at the same rate into the faster moving carrier stream results in a string of *longer* "high" and "low" concentration pulses. Their interaction with the surface will result in *lower* perceived frequency. As it turns out, the two effects always cancel out and the encoding frequency remains constant. The analogy of this conclusion is the constant pitch of a sound independent of the velocity of the wind (suggested by the reviewer).[8] This conclusion

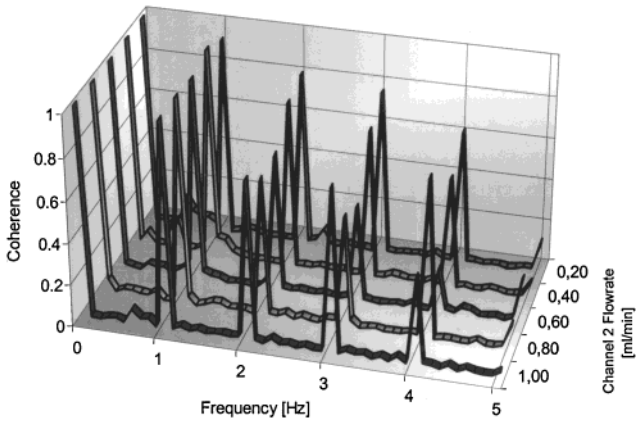

Figure 6. Dependence of the frequency on flow rate. The flow rate in channel 1 was 1.0 mL/min, while the flow rate in channel 2 varied from 0.2 to 1.0 mL/min. Coherence spectra are plotted against the flow rate of the channel 2. The modulation frequency was 1 Hz, and L_1 and L_2 were equal to 10 and 20 cm, respectively.

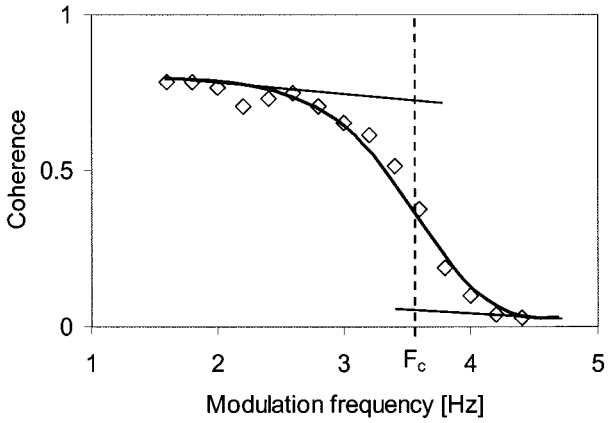

Figure 7. Determination of the fluidic bandwidth. Coherence values at the modulation frequency are plotted against the value of the modulation frequency. The modulation frequency was varied from 1.6 to 4.4 Hz. The delay elements L_1 and L_2 were 40 and 50 cm, respectively. Flow rate was 0.6 mL/min.

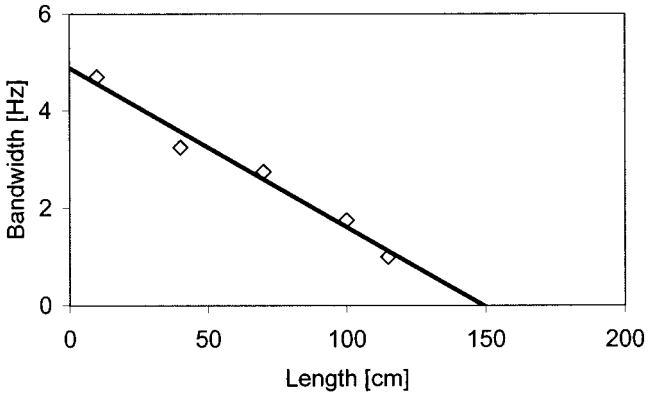

Figure 8. Dependence of the fluidic bandwidth on the distance from the source. (L_1 was used as distance of the array from the source.) The value of the fluidic bandwidth is plotted for L_1/L_2 pairs of 10/20, 40/50, 70/80, 100/110, and 115/125 cm, respectively. Flow rate was 0.6 mL/min.

has been confirmed experimentally. The flow in the channel one was kept constant at 1.0 mL/min while the flow in channel two was varied from 1.0 to 0.2 mL/min (8.2 to 1.6 cm/s). These flow rates are in the range of linear flow velocities of the turbulent flow conditions used for the LIF experiments (average flow rate 5 cm/s). Figure 6 shows that the fundamental modulation frequency stays constant over the whole range of flow rates. Therefore, we can state that *the frequency encoded in the plume structure does not depend on the flow rate in the individual channels.*

It is most remarkable that the coherence value at the fundamental frequency also does not depend on flow rate. Since the mass transport constant *m* (eq 2) depends on the local velocity vector at the sensor only, the amplitude of the received signal depends on the flow rate. The coherence function is, however, the correlated part of the signals normalized by the power of those signals. Therefore, it is independent of the intensity of the signals. On the other hand, coherence values at higher harmonics show some variations with changing flow. It is understandable since the origin of the higher harmonics lies in the nonsinusoidal (i.e., nonideal) shape of the concentration pulse. That distortion is difficult to control because it is changing with the flow velocity in a complex manner.[15]

Experimental Bandwidth. As we can see from the previous sections (Figure 5), the coherence value becomes lost in the noise at some finite distance from the source. A visual inspection of the plume also reveals the fact that the plume becomes more homogeneous, i.e., that the higher frequency components gradually disappear with distance. This effect can be qualitatively explained by the fact that diffusion smoothes the high-frequency variations. To prove this effect, the modulation frequency was varied from 1.6 to 4.4 Hz and coherence values were calculated for various delay element pairs of 10−20, 40−50, 70−80, 100−110, and 190−200 cm.

Figure 7 shows that for the same delay element pair (40−50 cm) coherence at the fundamental frequency stays initially constant and then starts decreasing with increasing frequency of the encoded signal. The critical value (F_c) is defined again as the frequency at the inflex of this experimental curve. This critical value also defines the *fluidic bandwidth* (FB) for the particular lengths of the delay element pair. The data in Figure 7 show that the frequency of chemical modulation at the distance of 40 cm from the modulation source is limited to frequencies below ~4.5 Hz. The FB values for different delay element pairs were then plotted against the length of the shorter delay element in the pair in Figure 8. This relationship shows what range of fundamental frequencies can be expected at certain distances from the source.

The above result seems to be in contradiction to the result shown in Figure 4 where the higher harmonic frequencies up to 6 Hz are discernible for the same length of delay lines. The important difference lies in the fact that these are higher harmonics that have a different physical meaning in this fluidic experiment. They are values of coherence observed at real frequencies. However, they result from nonidealities riding on top of the fundamental modulation frequencies. The fact that they can be observed and recorded means that the *signal bandwidth* could be wider than the *fluidic bandwidth.*

CONCLUSIONS

The results of our study prove unequivocally that information can be encoded in liquid flow in form of frequency and retrieved

(15) Taylor, G. I. *Proc. R. Soc. London A* **1953**, *219*, 186−203.

as coherence. The present results are limited to flows that are constrained in tubes and are mostly laminar. The only points of turbulence in our experiments are the mixing T-junction and the amperometric flow-through cells. Preliminary analysis of the LIF open plume data suggests that the multisensing/correlation analysis approach is indeed feasible.[9] Whether the marine animals in their chemotactic search algorithms can interpret it remains an open question at this point. The present study also confirms that multichannel chemical sensing performed with a sensing array allows a correlation and coherence analysis. The coherence is a robust parameter capable of revealing the encoded chemical information up to 4 Hz and a distance of up to 2 m. The distance at which the modulation can be detected is inversely proportional to the modulation frequency (Figure 8). Most importantly, this form of encoding is immune to changes in flow velocity.

Inexpensive, benchtop fluidic experiments (virtual plume) can yield useful information about the behavior of sensing arrays in complex flow conditions. This methodology has been used to perform more complex experiments, including multifrequency modulations and measurements in progressively more turbulent flows. The results of this research are reported in part 2 of this series.

ACKNOWLEDGMENT

The authors acknowledge helpful discussions and comments in the area of biology (M.J. Weissburg, D.B. Dusenbery), fluid mechanics (P.J.W. Roberts), and signal processing (P. Janata). The support for this work has been provided by DARPA/ONR Project N00014-98-1-0776.

Received for review February 14, 2001. Accepted June 4, 2001.

AC0101813